Letter

Structure−Activity Relationship Study of Splicing Modulators on Hsh155/SF3B1 through Chemical Synthesis and Yeast Genetics

Jacob P. Beard, Sierra L. Love, John C. Schmitz, Aaron A. Hoskins, and Kazunori Koide*

Cite This: *ACS Med. Chem. Lett.* 2024, 15, 2225−2230

Read Online

ACCESS | Metrics & More | Article Recommendations | SI Supporting Information

ABSTRACT: Meayamycins are synthetic analogs of the natural product FR901464 and exhibit potent anticancer activity against human cancers. They bind SF3B1 and PHF5A, components of the human spliceosome, and they alter pre-mRNA splicing. Detailed analysis of the active site led us to investigate a narrow pocket within the binding site that surrounds the α,β-unsaturated amide portion of meayamycin. We describe the synthesis and biological activity of two new analogs bearing a methyl substituent on the α or β position of the amide. With these analogs, we investigated the discrete interactions within the narrow region of SF3B1 using a human/yeast chimeric SF3B1 protein and found that the V1078 residue of SF3B1 affects compound binding at the amide moiety.

KEYWORDS: *structure−activity relationship, splicing, SF3B1, alternative splicing, anticancer activity*
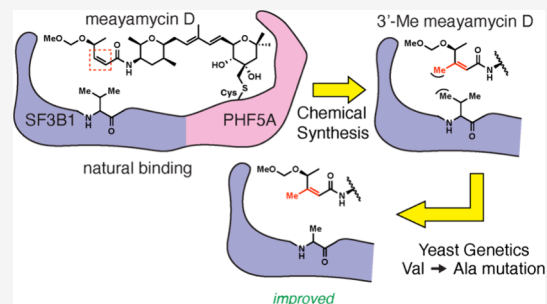
FR901464 was isolated from *Burkholderia* sp. FERM BP-3421 as an anticancer agent with half-maximal growth inhibition (GI_{50}) values of 1−2 nM against human cancer cells.[1−4] The molecule binds to human splicing factor 3B subunit 1 (SF3B1), a component of the human spliceosome, to inhibit precursor mRNA splicing.[5] Pladienolide B,[6−8] herboxidiene,[9−13] and other similar natural products[14,15] were also discovered from natural sources and found to bind to SF3B1 and inhibit splicing.[16,17] The isolations and biological activities of these natural products have sparked broad interest in the development of therapeutically useful pre-mRNA splicing inhibitors. FR901464 and closely related analogs have been synthesized and biologically evaluated by many groups.[18−27] The Kitahara group synthetically prepared spliceostatin A (SSA), a more stable 1-methoxy derivative of FR901464 (Figure 1).[20] After the initial discovery of SF3B1 as the relevant target of FR901464, the Pena group reported the cryo-EM structure of an SSA-bound SF3B complex, a large protein assembly that contains SF3B1 and other SF3B subunits. This structure revealed how the majority of the SSA molecule is bound by SF3B1 near the protein's interface with another SF3B subunit, plant homeodomain-finger domain 5A (PHF5A).[28] The structure showed that SSA forms a covalent adduct between the epoxide of SSA and the C26 of PHF5A.

Structure−activity relationship (SAR) studies of FR901464 have primarily focused on the two tetrahydropyran rings, diene moiety, and the C4' position.[18,25−27,29−37] In the cryo-EM structure of the SSA-SF3B1 complex, the enamide occupied the narrow neck region of the protein pocket (Figure 2). To gain additional insights, we decided to study the SAR around the C2' and C3' positions of FR901464 with our more metabolically stable analog, meayamycin D.[38] The region
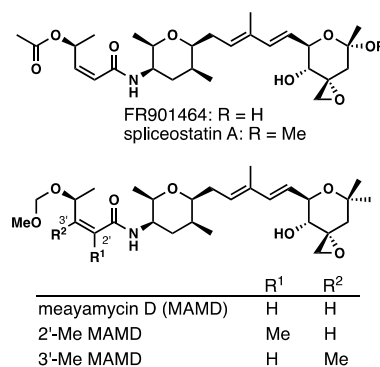
Figure 1. Structures of FR901464 (natural product) and synthetic analogs.

	R¹	R²
meayamycin D (MAMD)	H	H
2'-Me MAMD	Me	H
3'-Me MAMD	H	Me

between L1066 and V1078 residues of human SF3B1 appear to interact with the C2' and C3' positions of SSA. We previously compared the Z-enamide (naturally occurring) to the E-enamide and the C2'-C3' saturated equivalent.[39] The latter two compounds were found to be significantly less potent, indicating a possible steric constraint on the C3' position as well as preference for a rigid C2'-C3' bond.
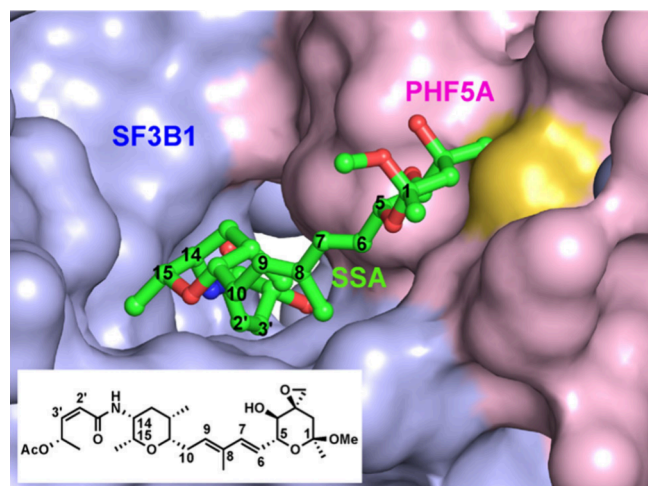
Figure 2. SF3B1 binding pocket occupied by SSA (PDB: 7B9C).

Herein, we report the synthesis and biological evaluation of two new analogs with an additional methyl group at the C2' or C3' position. The analogs were evaluated for their antiproliferative activity, splicing activity, and in vitro plasma stability. We reveal that the C3' substitution is tolerated and leads to a compound with comparable activity to meayamycin D. Lastly, we introduced several mutations into the SF3B1 binding site to understand the discrete interactions at the C2' and C3' site that may be required for compound activity.

The synthesis of 2'-Me meayamycin D began with **1**, which was prepared in a single step from commercially available ethyl-(S)-lactate (Scheme 1).[38] Sequentially, lactate **1** was reduced with diisobutylaluminum hydride (DIBALH), and the in situ-generated aldehyde was submitted to an Ando-Horner-Wadsworth-Emmons reaction[40] with phosphonate **9**[41] to yield the α-methylated enoate **2** in 52% yield, with an E/Z ratio of 6:94. Enoate **2** was hydrolyzed to acid **3** in a quantitative yield. To confirm the correct configuration, we reduced enoate **2** using DIBALH to allylic alcohol **8** in 68% yield. One-dimensional nuclear Overhauser effect (NOE) signals were detected for the C1' and C4' positions (Figure S1), confirming the Z-olefin geometry.[42] Acid **3** was coupled with amine **10**[42] to afford amide **4** as an inseparable mixture of isomers. The desired compound could be purified after olefin cross-metathesis with methacrolein, using the nitro-Grela catalyst,

to give aldehyde **5** in 39% yield over two steps. Wittig olefination of aldehyde **5** with Ph$_3$P=CH$_2$ gave diene **6** in 78% yield. Finally, this diene was united with fragment **7** to afford 2'-Me meayamycin D in 8% yield.

The synthesis of 3'-Me meayamycin D started with the hydrolysis of **1** to acid **11** in 84% yield (Scheme 2). Acid **11** was treated with trimethylacetyl chloride followed by N,O-dimethylhydroxylamine to give Weinreb amide **12** in 83% yield. Attempts to directly convert ester **1** to amide **12** failed. Grignard addition of in situ-generated MeMgI to amide **12** gave ketone **13** in 88% yield, which was directly subjected to an Ando-Horner-Wadsworth-Emmons olefination with phosphonate **20** in the presence of KO^{t}Bu to afford the β-methylated enoate **14** in 50% yield, with an E/Z ratio of 15:85. The olefin geometry of enoate **14** was confirmed using the same method as that for enoate **2**. Reduction of enoate **14** using DIBALH gave allylic alcohol **19** in 79% yield. Correlating NOE signals were observed between the C1' and C4' positions, indicating a Z-olefin geometry (Figure S2). Next, enoate **14** was hydrolyzed to acid **15** quantitatively, which was coupled with amine fragment **10** to afford amide **16** as an inseparable mixture of isomers. In a similar fashion, the desired compound was separated after olefin cross-metathesis with methacrolein, using nitro-Grela catalyst, to afford aldehyde **17** in 32% yield over two steps. Wittig olefination of aldehyde **17** with Ph$_3$P = CH$_2$ gave diene **18** in an 82% yield. Cross olefin metathesis of diene **18** with the right fragment **7** gave 3'-Me meayamycin D in 8% yield.

With 2'-Me meayamycin D and 3'-Me meayamycin D in hand, we evaluated the antiproliferative activity of the compounds in several human cancer cell lines (Table 1 and Figure S3). 2'-Me meayamycin D was significantly less potent with a GI$_{50}$ of 127−240 nM. Compared to the nonsubstituted analog, meayamycin D, this is approximately 2 orders of magnitude less potent.[38] During this work, the Arisawa group reported the synthesis and activity of a similar 2'-methylpentenamide derivative.[43] In their study, they reported that the 2'-methylpentenamide derivative gave less inhibitory activity against androgen receptor splice variant 7 (AR-V7) expression, as compared to SSA. As mentioned above, the crystallographic data suggest that this position lies in a relatively narrow space within the protein binding site. Given this, it is possible that the lower antiproliferative activity is due to steric clash between the C2'-methyl and the protein binding

Scheme 1. Synthesis of 2'-Me Meayamycin D[a]
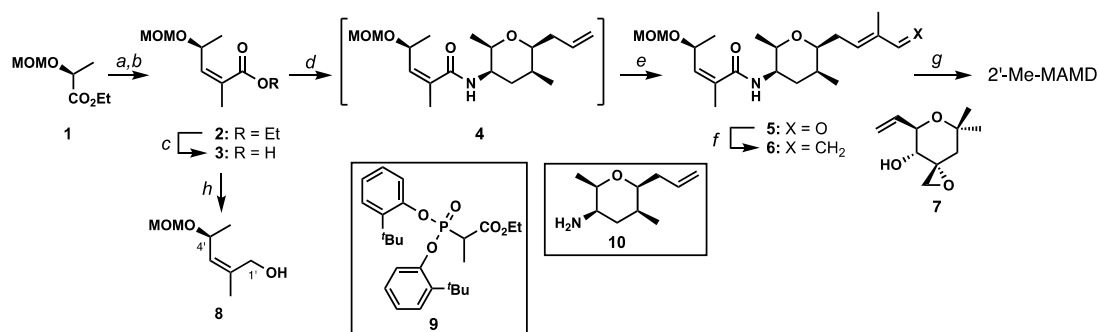
[a]Conditions: (a) diisobutylaluminum hydride (DIBALH), CH$_2$Cl$_2$, −78 °C, 2 h; then (b) **9**, KO^{t}Bu, tetrahydrofuran (THF), −78 °C to rt, 20 h, 52% (E:Z = 6:94); (c) NaOH, MeOH, 0 °C to rt, 16 h, quant.; (d) **10**, HATU, diisopropylethylamine, CH$_2$Cl$_2$, 0 °C to rt, 42 h, inseparable mixture; (e) methacrolein, nitro-Grela catalyst, 50 °C, 20 h, 39% for 2 steps; (f) Ph$_3$PCH$_3$Br, KO^{t}Bu, THF, 0 °C to rt, 18 h, 78%; (g) **7**, nitro-Grela catalyst, dichloroethane (DCE), 50 °C, 8 h, 8%; (h) DIBALH, THF, −78 °C, 1.5 h, 68%.

Scheme 2. Synthesis of 3′-Me Meayamycin D[a]
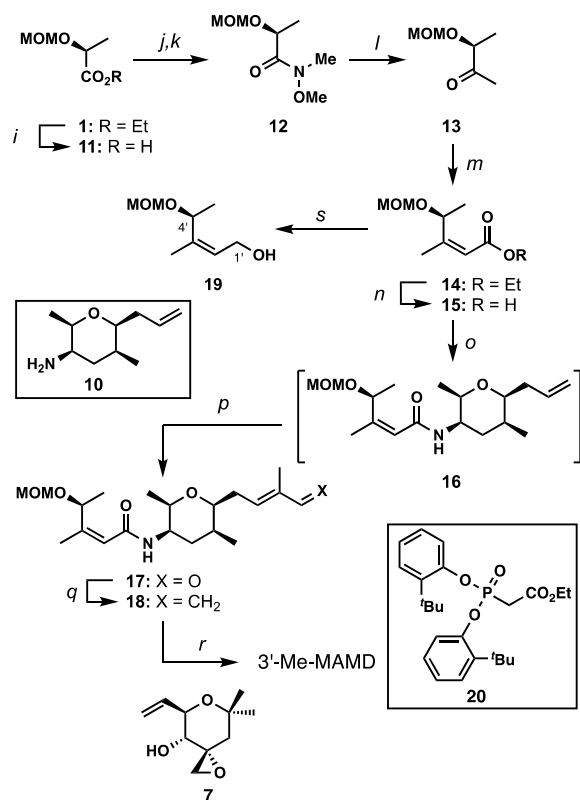
[a]Conditions: (i) LiOH, MeOH, H_2O, 3 h, 0 °C, 84%; (j) trimethylacetyl chloride, triethylamine, CH_2Cl_2, 0 °C, 1.5 h; then (k) N,O-dimethylhydroxylamine hydrochloride, triethylamine, CH_2Cl_2, 0 °C to rt, 20 h, 83%; (l) Mg, MeI, Et_2O, 0 °C, 2.5 h, 88%; (m) **20**, KO^{t}Bu, THF, 0 °C to rt, 18 h, 50% (E:Z = 15:85); (n) NaOH, MeOH, 0 °C, 3.5 h, quant.; (o) **10**, HATU, diisopropylamine, CH_2Cl_2, 0 °C to rt, 40 h, inseparable mixture; (p) methacrolein, nitro-Grela catalyst, 50 °C, 18 h, 32% for 2 steps; (q) Ph_3PCH_3Br, KO^{t}Bu, THF, 0 °C, 1.5 h, 82%; (r) **7**, nitro-Grela catalyst, DCE, 45 °C, 14 h, 8%; (s) DIBALH, THF, −78 °C, 2 h, 79%.

Table 1. Antiproliferative Activity of Meayamycin A, Meayamycin D, 2′-Me Meayamycin D, and 3′-Me Meayamycin D in Various Human Cancer Cell Lines[a]

	GI_{50} (nM)	
Cell lines	2′-Me meayamycin D	3′-Me meayamycin D
HCT116	129 ± 14	4.8 ± 0.9
SW48	127 ± 15	4.6 ± 0.7
A549	240 ± 48	7.2 ± 2.1
DMS53	169 ± 23	5.9 ± 1.0
DMS114	153 ± 20	5.5 ± 1.3

[a]Each value represents the average of $n \geq 3$ replicates, SD.

pocket of SF3B1. 3′-Me meayamycin D, is significantly more potent with GI_{50} of 4.6−7.2 nM. This suggests that methylation at the C3′ position is tolerated while methylation at the C2′ position results in a significant loss in activity.

We evaluated the ability of 2′-Me meayamycin D and 3′-Me meayamycin D to decrease the abundance of proteins whose expression is dependent on splicing of their respective pre-mRNAs (Figure 3). 3′-Me meayamycin D (GI_{50} = 5 nM) showed a comparable decrease in myeloid cell leukemia 1 (MCL-1) protein abundance to meayamycin D (GI_{50} = 2
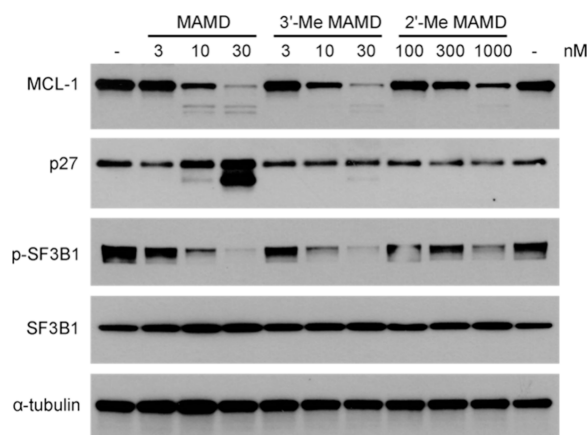

Figure 3. Western blot analysis of HCT116 cells treated with meayamycin D (MAMD), 3′-Me MAMD, and 2′-Me MAMD.

nM),[38] while 2′-Me meayamycin D (GI_{50} = 129 nM) showed only small changes in protein levels at concentrations up to 1 μM. Treatment with these analogs also led to a dose-dependent decrease of MCL-1 alternative splicing mirroring the expression levels of MCL-1, which has been previously observed in other meayamycin analogs (Figure S4).[44,45] These results corroborate the antiproliferative assay results and may serve as one explanation for the lower activity of 2′-Me meayamycin D. Interestingly, we observed a nearly negligible increase in a proteoform of p27 generated by alternative splicing of the coding pre-mRNA, as compared to meayamycin D. All compounds also lead to a decrease in SF3B1 phosphorylation, consistent with disruption of the splicing process.[46] Next, we investigated the stability of 2′-Me meayamycin D and 3′-Me meayamycin D in mouse CD1 plasma (Figure S5). 3′-Me meayamycin D has comparable stability in plasma compared to meayamycin D ($t_{1/2}$ = 13 h)[38] with a half-life of 16 h. Meanwhile, 2′-Me meayamycin D has a higher half-life of 30 h, which may be attributed to steric shielding of the amide bond.

To better understand the binding pocket for meayamycin D on SF3B1, we analyzed the crystal structure[28] and identified four residues that are near the C2′ and C3′ methyl group: L1066, R1074, T1077, and V1078 (Figure 4). We wondered whether the replacement of these residues with less bulky amino acids would improve the potency of the C2′-methylated analog. Using previously established methods,[47,48] we generated a human/yeast chimeric SF3B1 protein in S.
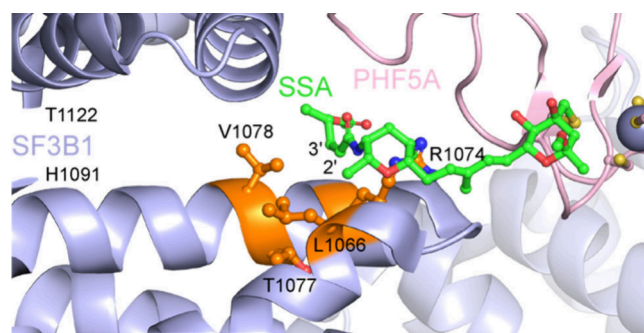
Figure 4. Proximal residues to the C2′ and C3′ position in the SSA-SF3B1 crystal structure (PDB: 7B9C, residues H1091−T1122 omitted for clarity).
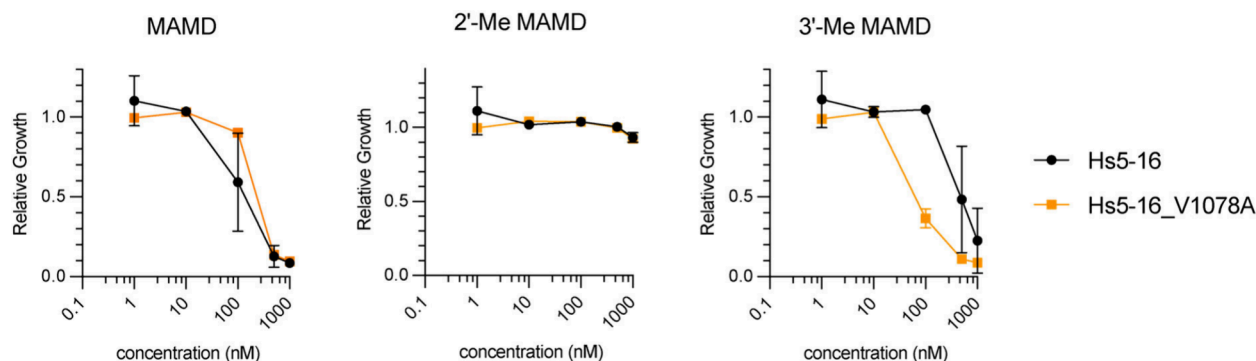
Figure 5. Growth inhibition of *S. cerevisiae* with chimeric Hs5−16 mutation V1078A in the presence of meayamycin D (MAMD), 2′-Me MAMD, and 3′-Me MAMD. Each point represents the average of *n* = 3 biological replicates, ± SD.

cerevisiae. The chimeric protein has HEAT domains 5−16 of the wild-type yeast SF3B1 (Hsh155) replaced with the human SF3B1 sequence (denoted as Hs5−16). We have previously shown these domains comprise the binding site for SSA and other small molecule splicing inhibitors and are responsible for the observed splicing effect of such compounds.[48] This chimera model provides a genetically tractable and facile way to detect splicing inhibition, since pre-mRNA splicing is essential in yeast. With this model in hand, we replaced the residues (L1066, R1074, T1077, V1078) with either alanine or glycine and compared the growth inhibition between meayamycin D, 2′-Me meayamycin D, 3′-Me meayamycin D, and herboxidiene (control) in *S. cerevisiae* with Hs5−16 (Figures S6 and S7). Meayamycin D has an approximate GI_{50} of 108 nM in unmodified Hs5−16, while 2′-Me meayamycin D does not inhibit growth at concentrations up to 1 μM (Figure S6, black curve). 3′-Me meayamycin D has a GI_{50} of 405 nM in Hs5−16, which is a trend similar to the observed activity of these compounds in human cancer cells. Both the L1066A and T1077A mutants were still inhibited by meayamycin D, albeit with less potency. Additionally, none of the selected mutations improved the compound activity of 2′-Me meayamycin D. One possibility is that the steric clash of the 2′-methyl may occur primarily between the protein backbone rather than the specific amino acids. In the case of L1066G, this residue lies close to the beginning of the α-helical fold. Therefore, replacement with the more flexible glycine may destabilize the α-helix and lead to decreased compound activity (although yeast can tolerate this substitution in an essential protein). This flexibility may also explain the observed weaker toxicity in the T1077G mutant as well for meayamycin D and 3′-Me meayamycin D. Notably, however, herboxidiene did not lose toxicity against the T1077G mutation (Figure S7). Finally, the V1078A mutant showed enhanced effect with 3′-Me meayamycin D with a GI_{50} of 80 nM (Hs5−16 GI_{50} = 405 nM; Figure 5), indicating that the valine at this position may be closer in proximity to the added 3′-methyl group.

In conclusion, we designed and synthesized two new analogs bearing methyl groups on the C2′ and C3′ positions. Our biological evaluation revealed that the C2′ position is not tolerated for substitution. In contrast, the C3′ substitution still retains modest activity compared to meayamycin D. 3′-Me meayamycin D inhibited the alternative splicing of *MCL-1* similar to meayamycin D, indicating these compounds likely behave similarly to affect cancer cell growth. Additionally, we investigated interactions within the SF3B1 binding pocket using a chimeric SF3B1 protein in yeast to understand the

binding of these substituted analogs. None of the mutants tested improved the ability of 2′-Me meayamycin D to inhibit growth, consistent with the intolerability for substitution at this position. Meanwhile, a V1078A mutant was identified to have enhanced activity with 3′-Me meayamycin D in comparison to both meayamycin D and the unmutated chimeric protein. The 3′-Me meayamycin D analog highlights a new position on FR901464-based compounds that is suitable for single carbon or single atom substitutions without a significant loss in potency and justifies further exploration of the binding pocket through structure−activity relationship studies.

■ ASSOCIATED CONTENT

Ⓢ Supporting Information

The Supporting Information is available free of charge at https://pubs.acs.org/doi/10.1021/acsmedchemlett.4c00510.

> Selective 1D NOE spectrum of compounds **8** and **19**; ^{1}H and ^{13}C{^{1}H} NMR spectrum of synthesized compounds; Antiproliferative assay data; RT-PCR; in vitro plasma stability; *S. cerevisiae* growth inhibition assays; detailed synthetic procedures; and general experimental protocols (PDF)

■ AUTHOR INFORMATION

Corresponding Author

Kazunori Koide − *Department of Chemistry, University of Pittsburgh, Pittsburgh, Pennsylvania 15260, United States; Cancer Therapeutics Program, UPMC Hillman Cancer Center, Pittsburgh, Pennsylvania 15232, United States;* Ⓞ orcid.org/0000-0001-8894-8485; Email: koide@pitt.edu

Authors

Jacob P. Beard − *Department of Chemistry, University of Pittsburgh, Pittsburgh, Pennsylvania 15260, United States;* Ⓞ orcid.org/0000-0002-3428-5345

Sierra L. Love − *Department of Biochemistry, University of Wisconsin—Madison, Madison, Wisconsin 53706, United States; Genetics Training Program, University of Wisconsin—Madison, Madison, Wisconsin 53706, United States;* Ⓞ orcid.org/0000-0003-3254-9009

John C. Schmitz − *Division of Hematology-Oncology, Department of Medicine, University of Pittsburgh School of Medicine, Pittsburgh, Pennsylvania 15232, United States; Cancer Therapeutics Program, UPMC Hillman Cancer Center, Pittsburgh, Pennsylvania 15232, United States;* Ⓞ orcid.org/0000-0001-6321-9606

Aaron A. Hoskins − *Department of Biochemistry, University of Wisconsin—Madison, Madison, Wisconsin 53706, United States; Department of Chemistry, University of Wisconsin—Madison, Madison, Wisconsin 53706, United States;* orcid.org/0000-0002-9777-519X

Complete contact information is available at:
https://pubs.acs.org/10.1021/acsmedchemlett.4c00510

Funding

Notes

The authors declare no competing financial interest.
Safety: No unexpected or unusually high safety hazards were encountered.

■ ACKNOWLEDGMENTS

■ ABBREVIATIONS

GI50, Half-maximal growth inhibition; MCL-1L, myeloid cell leukemia-1 long isoform; MCL-1S, myeloid cell leukemia-1 short isoform; SD, standard deviation; PHF5A, PHD finger protein 5A; SF3B1, splicing factor 3B subunit 1

■ REFERENCES

(1) Nakajima, H.; Sato, B.; Fujita, T.; Takase, S.; Terano, H.; Okuhara, M. New Antitumor Substances, FR901463, FR901464 and FR901465. I. Taxonomy, Fermentation, Isolation, Physico-Chemical Properties and Biological Activities. *J. Antibiot.* **1996**, *49* (12), 1196−1203.

(2) Nakajima, H.; Hori, Y.; Terano, H.; Okuhara, M.; Manda, T.; Matsumoto, S.; Shimomura, K. New Antitumor Substances, FR901463, FR901464 and FR901465. II. Activities against Experimental Tumors in Mice and Mechanism of Action. *J. Antibiot.* **1996**, *49* (12), 1204−1211.

(3) Nakajima, H.; Takase, S.; Terano, H.; Tanaka, H. New Antitumor Substances, FR901463, FR901464 and FR901465. III. Structures of FR901463, FR901464 and FR901465. *J. Antibiot.* **1997**, *50* (1), 96−99.

(4) Eustáquio, A. S.; Janso, J. E.; Ratnayake, A. S.; O'Donnell, C. J.; Koehn, F. E. Spliceostatin Hemiketal Biosynthesis in *Burkholderia* spp. is Catalyzed by an Iron/α-Ketoglutarate-Dependent Dioxygenase. *Proc. Natl. Acad. Sci. U.S.A.* **2014**, *111* (33), E337−E3385.

(5) Kaida, D.; Motoyoshi, H.; Tashiro, E.; Nojima, T.; Hagiwara, M.; Ishigami, K.; Watanabe, H.; Kitahara, T.; Yoshida, T.; Nakajima, H.; et al. Spliceostatin A Targets SF3b and Inhibits Both Splicing and Nuclear Retention of pre-mRNA. *Nat. Chem. Biol.* **2007**, *3* (9), 576−583.

(6) Sakai, T.; Sameshima, T.; Matsufuji, M.; Kawamura, N.; Dobashi, K.; Mizui, Y. Pladienolides, New Substances from Culture of *Streptomyces platensis* Mer-11107 I. Taxonomy, Fermentation, Isolation and Screening. *J. Antibiot.* **2004**, *57* (3), 173−179.

(7) Sakai, T.; Asai, N.; Okuda, A.; Kawamura, N.; Mizui, Y. Pladienolides, New Substances from Culture of *Streptomyces platensis* Mer-11107 II. Physico-Chemical Properties and Structure Elucidation. *J. Antibiot.* **2004**, *57* (3), 180−187.

(8) Mizui, Y.; Sakai, T.; Iwata, M.; Uenaka, T.; Okamoto, K.; Shimizu, H.; Yamori, T.; Yoshimatsu, K.; Asada, M. Pladienolides, New Substances from Culture of *Streptomyces platensis* Mer-11107 III. In vitro and in vivo Antitumor Activities. *J. Antibiot.* **2004**, *57* (3), 188−196.

(9) Isaac, B. G.; Ayer, S. W.; Elliott, R. C.; Stonard, R. J. Herboxidiene: A Potent Phytotoxic Polyketide from *Streptomyces* sp. A7847. *J. Org. Chem.* **1992**, *57* (26), 7220−7226.

(10) Millerwideman, M.; Makkar, N.; Tran, M.; Isaac, B.; Biest, N.; Stonard, R. Herboxidiene, a New Herbicidal Substance from *Streptomyces chromofuscus* A7847 - Taxonomy, Fermentation, Isolation, Physicochemical and Biological Properties. *J. Antibiot.* **1992**, *45* (6), 914−921.

(11) Edmunds, A. J. F.; Trueb, W.; Oppolzer, W.; Cowley, P. Herboxidiene: Determination of Absolute Configuration by Degradation and Synthetic Studies. *Tetrahedron* **1997**, *53* (8), 2785−2802.

(12) Sakai, Y.; Yoshida, T.; Ochiai, K.; Uosaki, Y.; Saitoh, Y.; Tanaka, F.; Akiyama, T.; Akinaga, S.; Mizukami, T. GEX1 Compounds, Novel Antitumor Antibiotics Related to Herboxidiene, Produced by *Streptomyces* sp. I. Taxonomy, Production, Isolation, Physicochemical Properties and Biological Activities. *J. Antibiot.* **2002**, *55* (10), 855−862.

(13) Sakai, Y.; Tsujita, T.; Akiyama, T.; Yoshida, T.; Mizukami, T.; Akinaga, S.; Horinouchi, S.; Yoshida, M.; Yoshida, T. GEX1 Compounds, Novel Antitumor Antibiotics Related to Herboxidiene, Produced by *Streptomyces* Sp II. The Effects on Cell Cycle Progression and Gene Expression. *J. Antibiot.* **2002**, *55* (10), 863−872.

(14) Liu, X.; Biswas, S.; Berg, M. G.; Antapli, C. M.; Xie, F.; Wang, Q.; Tang, M.-C.; Tang, G.-L.; Zhang, L.; Dreyfuss, G. Genomics-Guided Discovery of Thailanstatins a, B, and C as pre-mRNA Splicing Inhibitors and Antiproliferative Agents from *Burkholderia thailandensis* MSMB43. *J. Nat. Prod.* **2013**, *76* (4), 685−693.

(15) Zhao, Y.; Zhao, J.; Lu, C.; Zhang, H.; Qi, H.; Jiang, S.; Guo, X.; Wang, J.; Xiang, W. Two New Spliceostatin Analogs from the Strain *Pseudomonas* sp. HS-NF-1408. *J. Antibiot.* **2018**, *71* (7), 667−671.

(16) Kotake, Y.; Sagane, K.; Owa, T.; Mimori-Kiyosue, Y.; Shimizu, H.; Uesugi, M.; Ishihama, Y.; Iwata, M.; Mizui, Y. Splicing Factor SF3b as a Target of the Antitumor Natural Product Pladienolide. *Nat. Chem. Biol.* **2007**, *3* (9), 570−575.

(17) Hasegawa, M.; Miura, T.; Kuzuya, K.; Inoue, A.; Won Ki, S.; Horinouchi, S.; Yoshida, T.; Kunoh, T.; Koseki, K.; Mino, K.; et al. Identification of SAP155 as the Target of GEX1A (Herboxidiene), an Antitumor Natural Product. *ACS Chem. Biol.* **2011**, *6* (3), 229−233.

(18) Thompson, C. F.; Jamison, T. F.; Jacobsen, E. N. FR901464: Total Synthesis, Proof of Structure, and Evaluation of Synthetic Analogues. *J. Am. Chem. Soc.* **2001**, *123* (41), 9974−9983.

(19) Horigome, M.; Motoyoshi, H.; Watanabe, H.; Kitahara, T. A Synthesis of FR901464. *Tetrahedron Lett.* **2001**, *42* (46), 8207−8210.

(20) Motoyoshi, H.; Horigome, M.; Watanabe, H.; Kitahara, T. Total Synthesis of FR901464: Second Generation. *Tetrahedron* **2006**, *62* (7), 1378−1389.

(21) Fan, L.; Lagisetti, C.; Edwards, C. C.; Webb, T. R.; Potter, P. M. Sudemycins, Novel Small Molecule Analogues of FR901464, Induce Alternative Gene Splicing. *ACS Chem. Biol.* **2011**, *6* (6), 582−589.

(22) Ghosh, A. K.; Chen, Z. H. Enantioselective Syntheses of FR901464 and Spliceostatin A: Potent Inhibitors of Spliceosome. *Org. Lett.* **2013**, *15* (19), 5088−5091.

(23) Ghosh, A. K.; Veitschegger, A. M.; Sheri, V. R.; Effenberger, K. A.; Prichard, B. E.; Jurica, M. S. Enantioselective Synthesis of Spliceostatin E and Evaluation of Biological Activity. *Org. Lett.* **2014**, *16* (23), 6200−6203.

(24) Effenberger, K. A.; Urabe, V. K.; Prichard, B. E.; Ghosh, A. K.; Jurica, M. S. Interchangeable SF3B1 Inhibitors Interfere with pre-mRNA Splicing at Multiple Stages. *RNA* **2016**, *22*, 350.

(25) Yoshikawa, Y.; Ishibashi, A.; Murai, K.; Kaneda, Y.; Nimura, K.; Arisawa, M. Design and Synthesis of a Phenyl C-Glycoside Derivative

of Spliceostatin a and Its Biological Evaluation toward Prostate Cancer Treatment. *Tetrahedron Lett.* **2019**, *60* (51), 151313.

(26) Gartshore, C.; Tadano, S.; Chanda, P. B.; Sarkar, A.; Chowdari, N. S.; Gangwar, S.; Zhang, Q.; Vite, G. D.; Momirov, J.; Boger, D. L. Total Synthesis of Meayamycin and *O*-Acyl Analogues. *Org. Lett.* **2020**, *22* (21), 8714−8719.

(27) Yoshikawa, Y.; Ishibashi, A.; Takehara, T.; Suzuki, T.; Murai, K.; Kaneda, Y.; Nimura, K.; Arisawa, M. Design and Synthesis of 1,2-Deoxy-Pyranose Derivatives of Spliceostatin a toward Prostate Cancer Treatment. *ACS Med. Chem. Lett.* **2020**, *11* (6), 1310−1315.

(28) Cretu, C.; Gee, P.; Liu, X.; Agrawal, A.; Nguyen, T.-V.; Ghosh, A. K.; Cook, A.; Jurica, M.; Larsen, N. A.; Pena, V. Structural Basis of Intron Selection by U2 snRNP in the Presence of Covalent Inhibitors. *Nat. Commun.* **2021**, *12* (1), 4491.

(29) Motoyoshi, H.; Horigome, M.; Ishigami, K.; Yoshida, T.; Horinouchi, S.; Yoshida, M.; Watanabe, H.; Kitahara, T. Structure-Activity Relationship for FR901464: A Versatile Method for the Conversion and Preparation of Biologically Active Biotinylated Probes. *Biosci. Biotechnol. Biochem.* **2004**, *68* (10), 2178−2182.

(30) Lagisetti, C.; Pourpak, A.; Jiang, Q.; Cui, X.; Goronga, T.; Morris, S. W.; Webb, T. R. Antitumor Compounds Based on a Natural Product Consensus Pharmacophore. *J. Med. Chem.* **2008**, *51* (19), 6220−6224.

(31) Lagisetti, C.; Pourpak, A.; Goronga, T.; Jiang, Q.; Cui, X.; Hyle, J.; Lahti, J. M.; Morris, S. W.; Webb, T. R. Synthetic mRNA Splicing Modulator Compounds with in vivo Antitumor Activity. *J. Med. Chem.* **2009**, *52* (22), 6979−6990.

(32) Lagisetti, C.; Palacios, G.; Goronga, T.; Freeman, B.; Caufield, W.; Webb, T. R. Optimization of Antitumor Modulators of pre-mRNA Splicing. *J. Med. Chem.* **2013**, *56* (24), 10033−10044.

(33) Makowski, K.; Vigevani, L.; Albericio, F.; Valcárcel, J.; Álvarez, M. Sudemycin K: A Synthetic Antitumor Splicing Inhibitor Variant with Improved Activity and Versatile Chemistry. *ACS Chem. Biol.* **2017**, *12* (1), 163−173.

(34) Ghosh, A. K.; Veitschegger, A. M.; Nie, S.; Relitti, N.; MacRae, A. J.; Jurica, M. S. Enantioselective Synthesis of Thailanstatin A Methyl Ester and Evaluation of in Vitro Splicing Inhibition. *J. Org. Chem.* **2018**, *83* (9), 5187−5198.

(35) Nicolaou, K. C.; Rhoades, D.; Kumar, S. M. Total Syntheses of Thailanstatins A−C, Spliceostatin D, and Analogues Thereof. Stereodivergent Synthesis of Tetrasubstituted Dihydro- and Tetrahydropyrans and Design, Synthesis, Biological Evaluation, and Discovery of Potent Antitumor Agents. *J. Am. Chem. Soc.* **2018**, *140* (26), 8303−8320.

(36) Ghosh, A. K.; Reddy, G. C.; Kovela, S.; Relitti, N.; Urabe, V. K.; Prichard, B. E.; Jurica, M. S. Enantioselective Synthesis of a Cyclopropane Derivative of Spliceostatin A and Evaluation of Bioactivity. *Org. Lett.* **2018**, *20* (22), 7293−7297.

(37) Nicolaou, K. C.; Rekula, S. R.; Kumar, S. M.; Podilapu, A. R.; Matuszak, R. P.; Jung, P. M.; Lam, L. T.; Phillips, A. C.; Lyssikatos, J.; Munneke, S.; et al. Design, Synthesis, and Biological Investigation of Thailanstatin A and Spliceostatin D Analogues Containing Tetrahydropyran, Tetrahydrooxazine, and Fluorinated Structural Motifs. *J. Org. Chem.* **2021**, *86* (3), 2499−2521.

(38) Beard, J. P.; Bressin, R. K.; Markaj, P. L.; Schmitz, J. C.; Koide, K. Synthesis and Conformational Analysis of FR901464-Based RNA Splicing Modulators and Their Synergism in Drug-Resistant Cancers. *J. Med. Chem.* **2023**, *66* (21), 14497−14512.

(39) Osman, S.; Albert, B. J.; Wang, Y.; Li, M.; Czaicki, N. L.; Koide, K. Structural Requirements for the Antiproliferative Activity of Pre-mRNA Splicing Inhibitor FR901464. *Chem.—Eur. J.* **2011**, *17* (3), 895−904.

(40) Ando, K.; Oishi, T.; Hirama, M.; Ohno, H.; Ibuka, T. Z-Selective Horner-Wadsworth-Emmons Reaction of Ethyl (Diarylphosphono)Acetates Using Sodium Iodide and DBU. *J. Org. Chem.* **2000**, *65* (15), 4745−4749.

(41) Bressin, R. K.; Driscoll, J. L.; Wang, Y.; Koide, K. Scalable Preparation of Methylated Ando-Type Horner−Wadsworth−Emmons Reagent. *Org. Process Res. Dev.* **2019**, *23* (2), 274−277.

(42) Albert, B. J.; Sivaramakrishnan, A.; Naka, T.; Koide, K. Total Synthesis of FR901464, an Antitumor Agent That Regulates the Transcription of Oncogenes and Tumor Suppressor Genes. *J. Am. Chem. Soc.* **2006**, *128* (9), 2792−2793.

(43) Hirabayashi, S.; Tsuyuguchi, Y.; Li, Y.; Ohta, N.; Yoshikawa, Y.; Lin, B.; Fumimoto, M.; Nunomura, K.; Suzuki, T.; Haruta, J.; et al. Design and Synthesis of 4-Acetoxypentanamide Derivatives of Spliceostatin a and Their Biological Evaluation Towards Prostate Cancer Treatment. *Bioorg. Med. Chem. Lett.* **2023**, *91*, 129333.

(44) Gao, Y.; Koide, K. Chemical Perturbation of Mcl-1 Pre-mRNA Splicing to Induce Apoptosis in Cancer Cells. *ACS Chem. Biol.* **2013**, *8* (5), 895−900.

(45) Gao, Y.; Trivedi, S.; Ferris, R. L.; Koide, K. Regulation of HPV16 E6 and MCL1 by SF3B1 Inhibitor in Head and Neck Cancer Cells. *Sci. Rep.* **2014**, *4* (1), 6098.

(46) Wang, C.; Chua, K.; Seghezzi, W.; Lees, E.; Gozani, O.; Reed, R. Phosphorylation of Spliceosomal Protein SAP 155 Coupled with Splicing Catalysis. *Genes Dev.* **1998**, *12* (10), 1409−1414.

(47) Carrocci, T. J.; Paulson, J. C.; Hoskins, A. A. Functional Analysis of Hsh155/SF3b1 Interactions with the U2 snRNA/Branch Site Duplex. *RNA* **2018**, *24* (8), 1028−1040.

(48) Hansen, S. R.; Nikolai, B. J.; Spreacker, P. J.; Carrocci, T. J.; Hoskins, A. A. Chemical Inhibition of Pre-mRNA Splicing in Living *Saccharomyces cerevisiae. Cell Chem. Biol.* **2019**, *26* (3), 443−448.e3.